02

Luminescent cryothermometer based on $K_2YF_5:Er^{3+}$

© K.N. Boldyrev[1], M. Diab[1,2], N.M. Khaidukov[3], M.N. Popova[1]

[1] Institute of Spectroscopy, Russian Academy of Sciences, Troitsk, Moscow, Russia
[2] Moscow Institute of Physics and Technology (State University), Dolgoprudnyi, Moscow oblast, Russia
[3] Kurnakov Institute of General and Inorganic Chemistry, Russian Academy of Sciences, Moscow, Russia

e-mail: kn.boldyrev@gmail.com

Received October 17, 2023
Revised October 17, 2023
Accepted October 26, 2023

The luminescence spectra of the $K_2YF_5:Er^{3+}$ (0.5 at.%) were recorded in the spectral regions of the intermultiplet transitions ${}^4I_{13/2} \rightarrow {}^4I_{15/2}$ (region of about 1.5 μm, falling within the transparency window of a standard optical fiber) and ${}^4I_{11/2} \rightarrow {}^4I_{15/2}$ (region of about 0.98 μm) with high spectral resolution at different temperatures. Pairs of spectral lines are proposed for the implementation of a Boltzmann luminescent ratiometric cryothermometer in the temperature ranges of about 20, 40, and 60 K with a relative sensitivity of 8 to 3% K^{-1}. It is shown that measuring the half-width of a luminescence line with a wavelength of 1.538 μm (6500 cm^{-1}) provides a simple and reliable method for recording temperatures in the range from 20 to 90 K with a relative sensitivity of 3 to 2% K^{-1}.

Keywords: luminescence cryothermometry, $K_2YF_5:Er^{3+}$ crystal, high-resolution Fourier transform spectroscopy.

DOI: 10.61011/EOS.2023.10.57755.5735-23

Introduction

Luminescent thermometry is discussed as an intensively developing tool for remote temperature measurement (see, for example, the recent reviews [1–3] and the references therein). This method is used in such fields as chemical reactions, catalysis, microfluidics, micro- and nano-electronics, photonics, biology, and medicine. The temperature dependencies of various luminescence characteristics (namely, intensities, positions and widths of the bands, decay times) are used. The luminescence sources include diamonds with color centers, quantum dots in semiconductors, organic and hybrid phosphors, and micro- and nano-crystal with optically active ions of the transition elements. Presently, the temperature range within 100−800 K is well accommodated, some publications report about advancement to 20 K [4]. It should be noted in this context that detection of the temperatures below 20 K is important in aerospace studies, crystallographic synchrotron measurements, and for modern quantum technologies.

The low-temperature region shows small changes of the positions and widths of the luminescence lines, but their relative intensities can substantially change due to redistribution of populations of levels close in energy. So, the most suitable method for the low-temperature region is Boltzmann ratiometric thermometry [5]. In this case, excited states' levels separated by the energy interval $E_2-E_1=\Delta E$ are selected. Their equilibrium populations comply with the Boltzmann distribution $n_2(T)/n_1(T)=\exp(-\Delta E/kT)$. The relative intensities of the luminescence lines from the selected levels are measured:

$$R(T)=\frac{I_2(T)}{I_1(T)}=\frac{W_2 n_2(T)}{W_1 n_1(T)}=Ke^{(-\Delta E/kT)}. \qquad (1)$$

Here $K=W_2/W_1$ is the ratio of transition probabilities, which does not depend on the temperature (which, generally speaking, is not always fulfilled, so is neither the Boltzmann distribution [5]). Respectively, the absolute thermal sensitivity

$$S_a(T)=\frac{dR(T)}{dT} \qquad (2)$$

has a maximum at $T_m=\Delta E/2k$. Thermometers based on the different principles are compared using relative thermal sensitivity

$$S_r(T)=\frac{1}{R}\frac{dR(T)}{dT}. \qquad (3)$$

The Boltzmann ratiometric thermometers are the most attractively implemented by crystals containing rare-earth ions, whose energy spectrum consists of multiple narrow Stark levels with the different distances between them. The lower the temperatures being measured (T_m), the closer the levels of recording the luminescence lines, to be selected: $\Delta E \sim 2kT_m$ [5]. It is obvious that the smaller ΔE, the higher the spectral resolution required for spectrum recording.

The present paper has investigated applicability of the $K_2YF_5:Er^{3+}$ crystal as a luminescent ratiometric cryothermometer. It should be noted that the fluoride crystals doped with rare-earth ions are characterized by narrow lines of absorption and luminescence, thereby enabling transitions from the close levels, and by a significant density of phonon states at the low frequencies, which is favorable for establishing the Boltzmann distribution of the populations at the low temperatures. The K_2YF_5 fluoride crystals containing the rare-earth ions are known as effective Stokes and anti-Stokes phosphors, light frequency converters, materials for lasers and thermoluminescent dosimeters [6–14]. The Er^{3+} ion is selected due to the fact that this ion intensively

luminesces within a region of transparency window of fiber communication lines ($1.5\,\mu$m).

Experiment details

Procedure for preparation of crystal samples

Single crystals of the K_2YF_5 orthorhombic fluoride, which contain the Er^{3+} ions, have been produced in hydrothermal conditions. The hydrothermal experiments were conducted using autoclaves cladded by copper inserts, which have a volume of about 40 cm^3 and are separated by perforated diaphragms into a lower area of dissolution and an upper area of crystallization. The crystals were synthesized by a method of direct temperature gradient as a result of a reaction of aqueous solutions containing 40 mol.% KF, with a mixture of the oxides $0.995Y_2O_3$ and $0.005Er_2O_3$ at the temperature about 750 K, the reactor shell's temperature gradient about 3 K cm^{-1} and the pressure about 100 MPa. The purity of the oxides used was at least 99.99%. In these conditions, for 200 h, the autoclave crystallization area had spontaneously nucleated crystals of the size up to 0.5 cm^3synthesized. The produced crystals were transparent and pale rosy [15].

The small crystals were pulverized for X-ray diffraction analysis, while the bulky crystals were used to manufacture plates for the spectroscopy studies. The structure & phase composition of the produced samples was studied in a powder X-ray diffractometer Bruker D8 Advance with the monochromatic CuK_α-radiation. The X-ray patterns of the synthesized samples were analyzed by means of the EVA (Bruker) software package using the ICDD PDF-2 database for diffraction standards. All the diffraction reflexes identified from the samples are indicated in orthorhombic system with the lattice constants $a = 10.819$ Å, $b = 6.612$ Å, $c = 7.247$ Å. The reflexes also fully comply with peak positions of the standard card K_2YF_5 (JCPDS 01-072-2387). In other words, the X-ray diffraction analysis has confirmed that the lattice of the synthesized crystals belonged to the orthorhombic space group *Pnam* of the structural type K_2YF_5 [16]. The K_2YF_5 and K_2ErF_5 fluorides are isostructural compounds, while the ionic radii of the Y^{3+} and Er^{3+} ions have similar values, namely, 0.96 Å and 0.945 Å. Thus, it can be assumed that the concentrations of the Er^{3+} ions in the K_2YF_5 crystals correspond to the molar proportion Y_2O_3/Er_2O_3 in the initial mixture used for synthesizing the $K_2Y_{0.995}Er_{0.005}F_5$ crystals or at least these quantities are close in value.

Luminescence spectroscopy

The photoluminescence spectra of the $K_2YF_5:Er^{3+}$ crystal (0.5 at.%) at the various temperatures have been recorded on the Fourier-spectrometer Bruker IFS 125 HR with resolution of up to 0.01 cm^{-1} inside the spectral ranges of transitions from the levels of the Stark multiplets $^4I_{11/2}$ and $^4I_{13/2}$ to the levels of the ground multiplet $^4I_{15/2}$ (about 10 200 and 6500 cm^{-1}, respectively, or 0.98 and 1.54 μm in the wavelengths). They were recorded by using a luminescent attachment of an author design, CaF_2 as an interferometer's light divider, an InGaAs detector with a high amplification factor for spectrum recording. The crystal was cooled in a closed helium cycle cryostat Sumitomo SRP096 (3.5 → 90 K) with a step of 1 K. Luminescence was excited by a multi-mode diode laser of the power of 100 mW, with the wavelength of 809.4 nm and the spectrum width of 3.2 nm. At the same time, it was excited to the lower Stark level of the multiplet $^4I_{9/2}$ of the Er^{3+} ion [17]. The focus spot was 1 mm in diameter. Additional measures were taken to reduce the thermal load to the sample. They included the use of filters for attenuation of the excitation radiation, installation of a double polished cool screen with small openings for input and output of radiation. In addition to gluing the sample to a cryostat copper finger by a silver paste, the sample was also tightly wrapped in metal indium. The temperature was measured using a calibrated diode thermal sensor LakeShore DT-670 in close proximity to the sample and controlled and recorded using the temperature PID controller LakeShore Model 335. The temperature was controlled with the accuracy of ±0.05 K. The spectra recorded with the resolution of 0.01 cm^{-1} have been analyzed to show that the resolution of 0.1 cm^{-1} was enough to avoid spectrum distortion.

Results and discussion

Stark levels of the Er^{3+} ion in the $K_2YF_5:Er^{3+}$ crystal: Multiplets $^4I_{15/2}$, $^4I_{13/2}$, $^4I_{11/2}$

The information about the Stark structure of the levels of the Er^{3+} ion in the K_2YF_5 crystal was given in the paper [17] based on investigation of the absorption and luminescence spectra of the series of the solid solutions $K_2Y_{1-x}Er_xF_5$ ($0 < x \leq 1.0$). These data are given in the first column of Table 1. However, the paper [17] has failed to specify which erbium concentration and which temperature they belong to. Based on analysis of the high-resolution luminescence spectra of the $K_2YF_5:Er^{3+}$ (0.5 at.%) crystal, at the different temperatures (they are shown on the figures in the below sections) we have identified the spectral lines and determined the energies of the Stark levels in the multiplets $^4I_{15/2}$, $^4I_{13/2}$, $^4I_{11/2}$ of the ion Er^{3+} in the $K_2YF_5:Er^{3+}$ (0.5 at.%) crystal at the temperatures of 4 and 80 K (Table 1). Our data well comply with the data of the paper [17], excluding that we have failed to detect the levels with the energies of 35 and 37 cm^{-1}.

Photoluminescence within the region of the transition $^4I_{13/2} \rightarrow {}^4I_{15/2}$

Fig. 1, *a* shows the photoluminescence spectrum of the $K_2YF_5:Er^{3+}$ (0.5 at.%) crystal at the temperature of 50 K within the region of the transition $^4I_{13/2} \rightarrow {}^4I_{15/2}$ in the Er^{3+} ion under excitation by the diode laser with the

Table 1. Energies E of the Stark levels of the ion Er^{3+} in the $K_2YF_5:Er^{3+}$ crystal (0.5 at.%), as obtained from analysis of the luminescence spectra at the temperatures of 4 and 80 K

$^{2S+1}L_J$	№	E, cm^{-1} [17]	E, cm^{-1} $T = 4$ K This study	E, cm^{-1} $T = 80$ K This study
$^4I_{15/2}$	0	0	0	0
	1	34	34.8	34.3
	2	35	–	–
	3	37	–	–
	4	74	73.0	72.6
	5	111	111.0	110.1
	6	280	283.0	283.7
	7	502	500.6	500.1
$^4I_{13/2}$	*A*	6534	6534.5	6534.2
	B	6565	6565.8	6565.5
	C	6601	6601.4	6601.3
	D	6696	6695.0	6696.2
	E	6730	6729.6	6729.2
	F	6762	6762.0	6762.3
	G	6872	6871.2	6872.0
$^4I_{11/2}$	*A*	10233	10232.9	10232.5
	B	10260	10260.3	10260.1
	C	10302	10302.3	10301.8
	D	10317	10317.3	10316.6
	E	10340	10340.3	10340.4
	F	10397	10396.2	10396.7

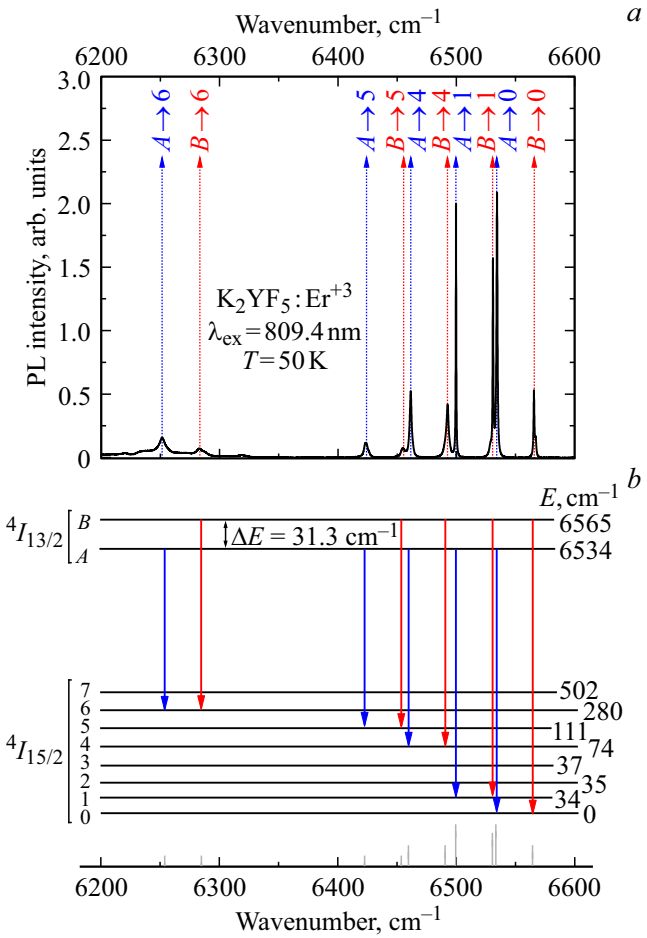

Figure 1. (*a*) Photoluminescence spectrum of the $K_2YF_5:Er^{3+}$ crystal (0.5 at.%) within the region of the transition $^4I_{13/2} \rightarrow {}^4I_{15/2}$ in the ion Er^{3+} at the temperature of 50 K, $\lambda_{ex} = 809.4$ nm; (*b*) Diagram of the levels that explains identification of the luminescence lines.

wavelength of 809.4 nm. The diagram of the levels of Fig. 1, *b* explains identification of the spectrum lines. At the temperature of 50 K, there is the populated level *B* that is separated by the slit $\Delta E = 31.3\,cm^{-1}$ from the level *A*, which is the lowest one in the multiplet $^4I_{13/2}$, and the luminescence spectrum exhibits lines corresponding to the transitions from this level (Fig. 1, *a*). The next level *C* is spaced from the level *A* already by $67\,cm^{-1}$ (Table 1) and is populated so poorly that you can not see the transitions therefrom. When measuring the relative intensities of the luminescence lines from the levels *B* and *A* with the distance $\Delta E = 31.3\,cm^{-1}$ between them, then it is possible to obtain the thermometer for the temperatures around $T_m = 22.5$ K (at $T_m = \Delta E/2k$ the absolute sensitivity is the highest).

Figure 2 clearly shows evolution of a high-frequency part of the spectrum with the temperature. With decrease in the temperature, the luminescence lines are noticeably narrowed; the population of the level *B* drops, while that of the level *A* — increases, thereby resulting in a decreased ratio of the intensities of the lines starting from the levels *B* and *A*. The decrease in the total intensity of the luminescence spectrum with decrease in the temperature is related to leaving the laser mode's resonance due to narrowing and shift of the Stark level of the Er^{3+} ion, which is excited.

Fig. 3, *a* shows the temperature dependency of the ratio $R(T)$ of the integral intensities of the lines $6455\,cm^{-1}$ [the transition $B(^4I_{13/2}) \rightarrow 5(^4I_{15/2})$] and $6424\,cm^{-1}$ [the transition $A(^4I_{13/2}) \rightarrow 5(^4I_{15/2})$]. It is clear that this dependency follows the Boltzmann distribution of the populations of the levels *B* and *A*, separated by the interval of $31.3\,cm^{-1}$. Figure 3, *b* illustrates the absolute and relative sensitivities depending on the temperature. The maximum absolute sensitivity is achieved at $T_m = 22.5$ K, while the relative sensitivity at this temperature is $8\%\,K^{-1}$. When the measurement accuracy for $R(T)$ is about 1% (as in our experiments), the resolved temperature interval is evaluated to be $\delta T \approx 0.12$ K.

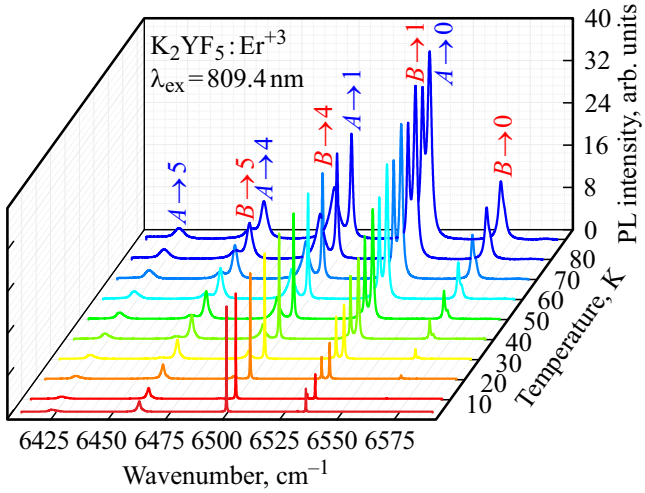

Figure 2. Photoluminescence spectra of the $K_2YF_5:Er^{3+}$ crystal (0.5 at.%) within the region of the transition $^4I_{13/2} \rightarrow {}^4I_{15/2}$ in the Er^{3+} ion within the temperature range of 3.5 → 90 K. $\lambda_{ex} = 809.4$ nm.

It should be noted that for pairs of luminescence lines starting from the levels B and A, to the levels $0, 1, 4$, the temperature dependency of the intensity ratio is deviated from the Boltzmann dependency, which seems to be related to the resonance absorption: the population of the levels $0, 1, 4$ varies with the temperature, whereas the level 5 is almost unpopulated up to 90 K.

Figure 3 shows that the relative intensity of luminescence from the levels separated by the interval of about 30 cm^{-1} creates a perspective for developing the thermometer with suitable characteristics for the temperature region near 20 K. The temperature range can be extended by measuring the half-width of the luminescence line. Fig. 4 shows the temperature dependency of the half-width (the full width at half height) of the line 6500 cm^{-1} [the transition $A(^4I_{13/2}) \rightarrow 1(^4I_{15/2})$]. The absolute sensitivity grows with increase in the temperature, whereas the relative sensitivity has a maximum about 3% K^{-1} at 30 K and drops to 2% K^{-1} at 90 K.

Photoluminescence within the region of the transition $^4I_{11/2} \rightarrow {}^4I_{15/2}$

The photoluminescence spectra within the region of the transition $^4I_{11/2} \rightarrow {}^4I_{15/2}$ are shown on Figures 5 and 6 together with the respective diagram of the levels (Fig. 5, *b*). Luminescence in this region is weaker than at the transition $^4I_{13/2} \rightarrow {}^4I_{15/2}$. The energy distance between the two lowest levels A and B of the multiplet $^4I_{11/2}$ $\Delta E = 27$ cm^{-1}, which is close to the above-discussed case $\Delta E = 31.3$ cm^{-1}. The level D is spaced from the lowest level A by 84 cm^{-1}: the pair of the lines 10 206 cm^{-1} [the transition $D(^4I_{11/2}) \rightarrow 5(^4I_{15/2})$] and 10 122 cm^{-1} [the transition $A(^4I_{11/2}) \rightarrow 5(^4I_{15/2})$] can be selected for the luminescent thermometry within the region about 60 K.

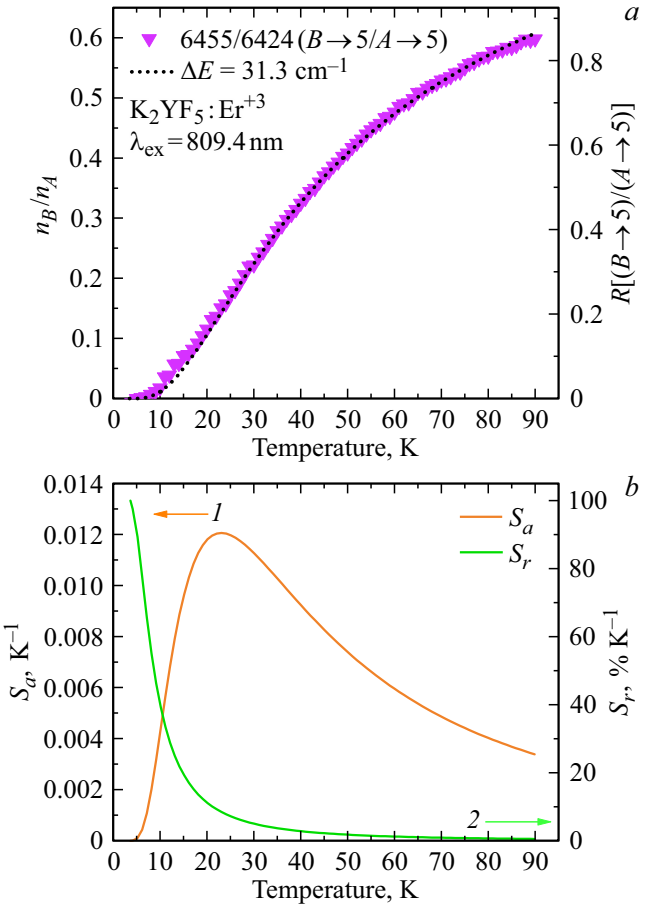

Figure 3. Temperature dependencies of (*a*) the ratio $R[(B \rightarrow 5)/(A \rightarrow 5)]$ of the integral intensities of the luminescence lines 6455 cm^{-1} [the transition $B(^4I_{13/2}) \rightarrow 5(^4I_{15/2})$] and 6424 cm^{-1} [the transition $A(^4I_{13/2}) \rightarrow 5(^4I_{15/2})$] (the symbols), and of the ratio of the populations n_B/n_A of the levels B and A, separated by the interval of 31.3 cm^{-1}, under the assumption of the Boltzmann distribution (the dashed line); (*b*) the absolute S_a (the orange curve *1*) and relative S_r (the green line *2*) sensitivities.

Fig. 7, *a* shows the temperature dependencies of the ratios of the integral intensities of these lines as compared to the ratio of the Boltzmann populations of the levels D and A. For the temperature region around 40 K, levels D and B with the distance of 57 cm^{-1} between them are suitable (Fig. 7, *b*).

The characteristics of the luminescent thermometers based on $K_2YF_5:Er^{3+}$ are provided in Table 2.

Conclusion

Applicability of the spectra of luminescence of the $K_2YF_5:Er^{3+}$ crystal has been studied for remote measurement of the low temperatures. The spectra of luminescence of the $K_2YF_5:Er^{3+}$ (0.5 at.%) crystal have been recorded at the various temperatures and under excitation by radiation

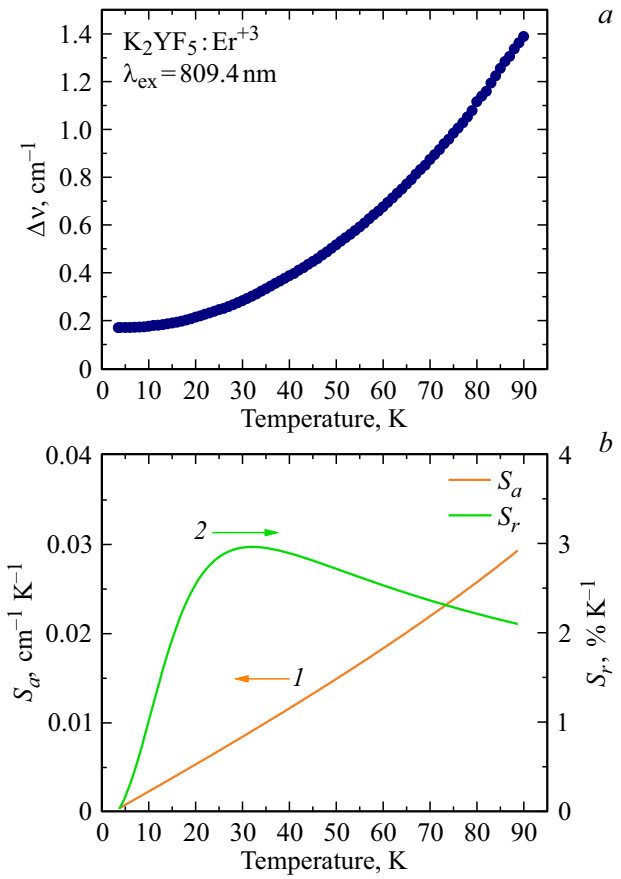

Figure 4. Temperature dependencies (a) of the half-width $\Delta\nu$ of the luminescence line 6500 cm^{-1} [the transition $A(^4I_{13/2}) \rightarrow 1(^4I_{15/2})$]; ($b$) of the absolute S_a (the orange curve *1*) and the relative S_r (the green curve *2*) sensitivities.

Table 2. Thermometric characteristics of the luminescent thermometers based on $K_2YF_5:Er^{3+}$

Optical parameter	λ, μm	T_m, K	S_r (T_m),% K^{-1}	δT, K
R [6454 cm^{-1}/6422 cm^{-1}]	1.557	22.4	8.0	0.12
$\Delta\nu$ of the line 6500 cm^{-1}	1.538	35 90	3.0 2.0	0.5 0.17
R [10206 cm^{-1}/10149 cm^{-1}]	0.985	41.0	5.0	0.8
R [10206 cm^{-1}/10122 cm^{-1}]	0.985	60.4	3.2	0.6

from the diode laser of the wavelength of 809.4 nm and the spectrum width of 3.2 nm. The crystal temperature was controllably changed from 3.5 to 90 K. Investigation of the infrared spectra within the region of the inter-multiplet transitions $^4I_{13/2} \rightarrow {}^4I_{15/2}$ (the wavelengths near 1.5 μm) and $^4I_{11/2} \rightarrow {}^4I_{15/2}$ (0.98 μm) was performed with high spectral resolution. Radiation with the wavelengths near 1.5 μm falls inside the transparency window of the optic fibers, which is especially valuable for purposes of remote probing.

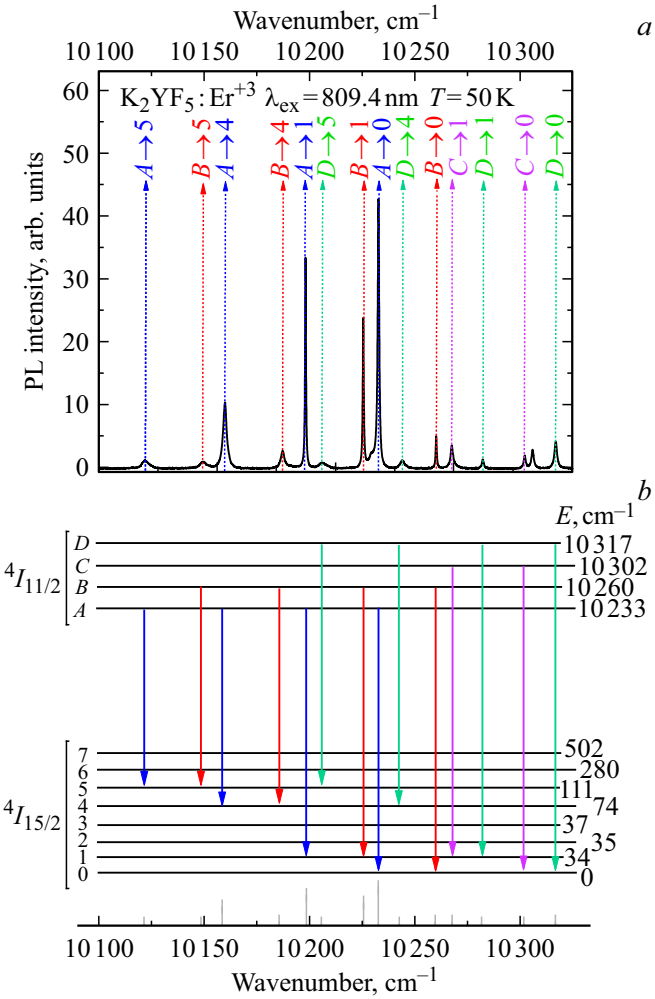

Figure 5. (a) Photoluminescence spectrum of the $K_2YF_5:Er^{3+}$ (0.5%) crystal within the region of the transition $^4I_{11/2} \rightarrow {}^4I_{15/2}$ in the Er^{3+} ion at the temperature of 50 K, λ_{ex} = 809.4 nm; (b) Diagram of the levels that explains identification of the lines.

We have also refined the diagram of the Stark levels of the Er^{3+} ion in the multiplets $^4I_{15/2}$, $^4I_{13/2}$ and $^4I_{11/2}$. Our data principally comply with the data of the paper [16], but from the levels of the ground multiplet with the energies of 34, 35 and 37 cm^{-1} only the level of 34 cm^{-1} has been recorded by us.

We have demonstrated that in order to implement the Boltzmann luminescent ratiometric cryothermometer, the pairs of the spectral lines 6454–6422 cm^{-1}, 10 206–10 149 cm^{-1} and 10 206–10 122 cm^{-1} are suitable, which correspond to the transitions from the pairs of the levels separated by the energy intervals of 31.3, 57 and 84 cm^{-1}, respectively. The respective temperatures at which the absolute sensitivity is the greatest, are 22.4, 41, and 60 K, while the relative sensitivities at these temperatures are 8, 5, and 3.2% K^{-1}.

The narrowest lines of luminescence are observed for the transitions between the lowest Stark levels of the multiplets, which are least of all prone to phonon relaxation. For

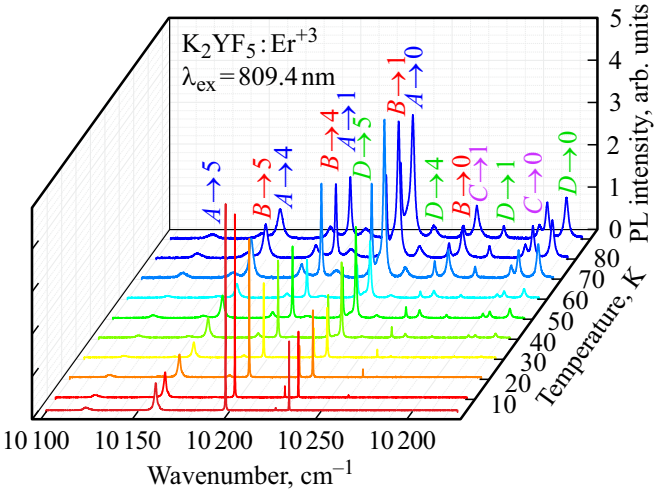

Figure 6. Photoluminescence spectra of the $K_2YF_5:Er^{3+}$ (0.5%) crystal within the region of the transition $^4I_{11/2} \to {}^4I_{15/2}$ in the Er^{3+} ion within the temperature range of 3.5 → 90 K. λ_{ex} = 809.4 nm.

the studied $K_2YF_5:Er^{3+}$ crystal, the half-width of these lines noticeably varies as the temperature changes in the temperature range above ~ 20 K. In particular, for the line of luminescence with the wavelength of 1.538 μm (6500 cm^{-1}), the half-width smoothly increases from 0.2 to 1.4 cm^{-1} within the temperature range from 20 to 90 K. We obtain the luminescent cryothermometer for this temperature region with slightly variable relative sensitivity (from 2 to 3% K^{-1}).

Funding

This study was supported financially by the Russian Science Foundation (the grant No. 23-12-00047). The measurements were carried out at the unique scientific unit „Multifunctional high-resolution wide-range spectroscopy“ (USU MHRWRS ISAS [18]).The crystals were synthesized and identified with support by the Ministry of Science and Higher Education of the Russian Federation within the state assignments of the Kurnakov Institute of General and Inorganic Chemistry. The studies were carried out using the equipment of Center for Collective Use of the SMPM in the Institute of General and Inorganic Chemistry of RAS.

Conflict of interest

The authors declare that they have no conflict of interest.

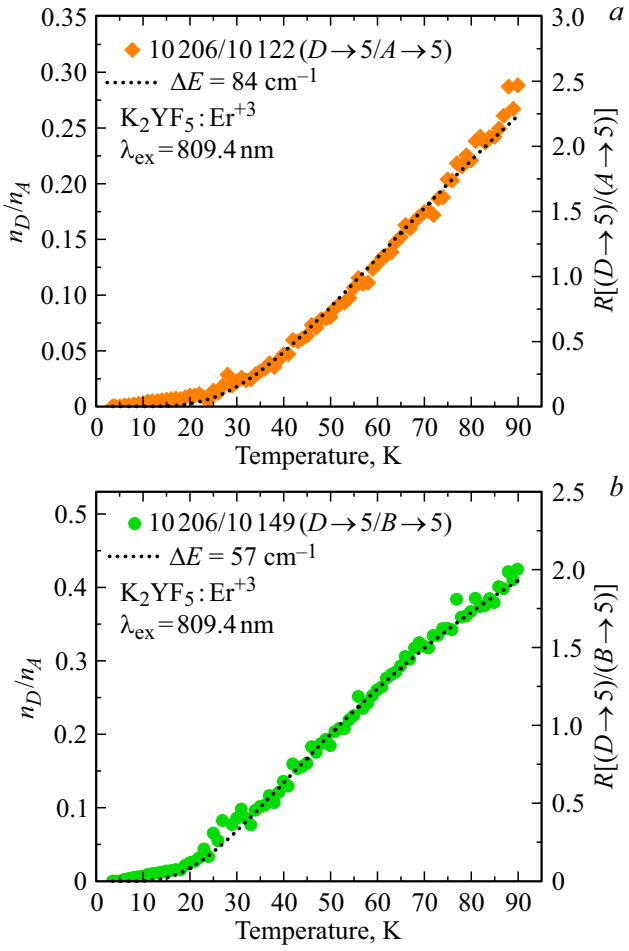

Figure 7. Temperature dependencies of the ratios of the integral intensities of the lines (*a*) 10 206 cm^{-1} [the transition $D(^4I_{11/2}) \to 5(^4I_{15/2})$] and 10 122 cm^{-1} [the transition $A(^4I_{11/2}) \to 5(^4I_{15/2})$]; (*b*) 10 206 cm^{-1} [the transition $D(^4I_{11/2}) \to 5(^4I_{15/2})$] and 10 149 cm^{-1} [the transition $B(^4I_{11/2}) \to 5(^4I_{15/2})$] (the symbols), and of the populations of the levels (*a*) *D* and *A*, separated by the interval of 84 cm^{-1}; (*b*) *B* and *A*, separated by the interval of 57 cm^{-1} under the assumption of the Boltzmann distribution (the dashed lines).

References

[1] L. Marciniak, K. Kniec, K. Elzbieciak-Piecka, K. Trejgis, J. Stefanska, M. Dramićanin. Coordination Chem. Rev., **469**, 21467 (2022). DOI: 10.1016/j.ccr.2022.214671
[2] M.D. Dramićanin. J. Appl. Phys., **128**, 040902 (2020). DOI: 10.1063/5.0014825
[3] C.D.S. Brites, S. Balabhadra, L.D. Carlos. Adv. Optical Mater., **2019**, *7*, 1801239 (2019). DOI: 10.1002/adom.201801239
[4] C.D.S. Brites, K. Fiaczyk, J.F.C.B. Ramalho, M. Sójka, L.D. Carlos, E. Zych. Adv. Optical Mater., **2018**, 1701318 (2018). DOI: 10.1002/adom.201701318
[5] M. Suta, A. Meijerink. Adv. Theory Simul., **2020**, *3*, 2000176 (2020). DOI: 10.1002/adts.202000176
[6] V.N. Makhov, N.M. Khaidukov. Nucl. Instrum. Methods Phys. Res. B, **308**, 205–207 (1991). DOI: 10.1016/0168-9002(91)90627-3
[7] Z. Kollia, E. Sarantopoulou, A.C. Cefalas, A.K. Naumov, V.V. Semashko, R.Y. Abdulsabirov, S.L. Korableva. Opt. Commun., **149**, 386–392 (1998). DOI: 10.1016/S0030-4018(97)00725-6
[8] P.V. Do, V.P. Tuyen, V.X. Quang, N.T. Thanh, V.T.T. Ha, N.M. Khaidukov, Y.I. Lee, B.T. Huy. J. Alloys Compd., **520**, 262–265 (2012). DOI: 10.1016/j.jallcom.2012.01.037

[9] T.J. Lee, L.Y. Luo, E.W.G. Diau, T.M. Chen, B.M. Cheng, C.Y. Tung. Appl. Phys. Lett., **89**, 131121 (2006). DOI: 10.1063/1.2358193
[10] J. Azorín-Nieto, M.N. Khaidukov, A. Sánchez-Rodriguez, J.C. Azorín-Vega. Nucl. Instrum. Methods Phys. Res. B, **263**, 36–40 (2007). DOI: 10.1016/j.nimb.2007.04.082
[11] D. Wang, M. Yin, S. Xia, V.N. Makhov, N.M. Khaidukov, J.C. Krupa. J. Alloys Compd., **368**, 337–341 (2004). DOI: 10.1016/j.jallcom.2003.08.061
[12] H.K. Hanh, N.M. Khaidukov, V.N. Makhov, V.X. Quang, N.T. Thanh, V.P. Tuyen. Nucl. Instrum. Methods Phys. Res. B, **268**, 3344–3350 (2010). DOI: 10.1016/j.nimb.2010.06.041
[13] J. Azorín, A. Gallegos, T. Rivera, J.C. Azorín, N.M. Khaidukov. Nucl. Instrum. Methods Phys. Res. A, **580**, 177–179 (2007). DOI: 10.1016/j.nima.2007.05.077
[14] A. Kadari, R. Mostefa, J. Marcazzo, D. Kadri. Radiat. Protect. Dosim., **167** (2015) 437–442. DOI: 10.1093/rpd/ncu364
[15] J. Méndez-Ramos, P. Acosta-Mora, J.C. Ruiz-Morales, N.M. Khaidukov. J. Alloys Compd., **575**, 263–267 (2013). DOI: 10.1016/j.jallcom.2013.04.014
[16] F. Loncke, D. Zverev, H. Vrielinck, N.M. Khaidukov, P. Matthys, F. Callens. Phys. Rev. B, **75**, 144427 (2007). DOI: 10.1103/PhysRevB.75.144427
[17] R.E. Peale, H. Weidner, F.G. Anderson, N.M. Khaidukov. OSA Trends in Optics and Photonics Series Vol. 10 Advanced Solid State Lasers. C.R. Pollock and W.R. Bosenberg (eds) (Optica Publishing Group, 1997). p. 462–466. DOI: 10.1364/ASSL.1997.SC14
[18] https://ckp-rf.ru/catalog/usu/508571/

Translated by M.Shevelev